Algorithmic lattice kirigami: A route to pluripotent materials

Daniel M. Sussman[a,1], Yigil Cho[a,b,1], Toen Castle[a], Xingting Gong[a], Euiyeon Jung[b], Shu Yang[b], and Randall D. Kamien[a,2]

[a]Department of Physics and Astronomy, University of Pennsylvania, Philadelphia, PA 19104; and [b]Department of Materials Science and Engineering, University of Pennsylvania, Philadelphia, PA 19104

Edited by Sharon C. Glotzer, University of Michigan, Ann Arbor, MI, and approved April 30, 2015 (received for review March 26, 2015)

We use a regular arrangement of kirigami elements to demonstrate an inverse design paradigm for folding a flat surface into complex target configurations. We first present a scheme using arrays of disclination defect pairs on the dual to the honeycomb lattice; by arranging these defect pairs properly with respect to each other and choosing an appropriate fold pattern a target stepped surface can be designed. We then present a more general method that specifies a fixed lattice of kirigami cuts to be performed on a flat sheet. This single pluripotent lattice of cuts permits a wide variety of target surfaces to be programmed into the sheet by varying the folding directions.

topological defects | origami | pluripotent

Reduced-dimensionality objects can be light yet extremely strong, as in a geodesic dome or the skeleton of a diatom (1). Design of such structures couples scale-independent geometry and topology with material properties to create a variety of structures. In soft gel sheets, programmed inhomogeneous swelling and stretching can generate tunable 3D shapes that can potentially serve as compliant mechanisms (2). In more rigid systems, origami applies a prescribed sequence of folds to a flat sheet and returns a strong, lightweight, and flexible 3D structure. A great deal of effort has gone into exploring the breadth of attainable origami surfaces starting from nearly unstretchable sheets (3–5), including recent work on designing mechanical metamaterials (6) and self-folding origami structures (7).

In origami, the inverse problem of prescribing a set of folds to achieve a target structure has been algorithmically solved. For instance, the circle/river packing method can be used to create a 2D base for the final product which is then augmented with extra folds into the desired 3D shape (8). A different method wraps the initial flat sheet onto a polygonally tiled target surface, using tucking molecules to hide the excess material within the final shape, and thus creates curvature (9). Further, software has been developed by the same author to form developable, irregularly corrugated target configurations by modifying miura-ori–style patterns (10).

There are, nevertheless, certain limits and constraints in the use of origami to design generic structures. These problems center around the potential complexity of the initial fold pattern and the subsequent greatly magnified complexity of the required sequence of folds along this pattern. For instance, the fold patterns specified by the circle/river packing algorithms return a pattern whose folded state matches a target surface, but there is no guarantee that any subset of creases can be folded; complex models of this type are typically precreased and then folded in a very specific and repetitive sequence. The polygonally tiled surfaces created by the tucking molecule method are the product of intricately interlocking crimp folds hidden away beneath the surface. Both of these features reflect the fact that typically complex origami designs do not permit a monotonic, continuous folding motion from the planar state to the desired target state. These extremely delicate fold patterns present an obvious challenge to the goal of designing self-assembling origami structures, where in many cases extremely fine control of the fold ordering may be required. Additionally, these fold patterns often waste much of the surface to create effective areas of Gaussian curvature, using extremely intricate folds, wedges, and pleats to effectively remove material, hiding it beneath the visible surface.

Recently, we introduced lattice kirigami methods to this design problem (11); inspired by the work of Sadoc, Rivier, and Charvolin on phyllotaxis (12–14), we supplemented the folds of origami with a limited set of cutting and regluing moves taking place on a honeycomb lattice (11). The essence of our kirigami constructions is that after making the prescribed cuts and identifying edges we have a surface with localized points of Gaussian curvature, which cause the surface to buckle into a 3D configuration. Associated folding then precisely defines the shape of the surface, corralling the points of Gaussian curvature into useful cues that direct the shape of the final structure.

The restrictions imposed on kirigami by the honeycomb lattice and its triangular dual lattice led to a manageable set of allowed motifs: 2–4 disclination pairs on the honeycomb lattice and $\tilde{5}$–$\tilde{7}$ disclination pairs on the dual lattice (dual lattice constructs are denoted by tildes) that could be connected to other disclination pairs with cancelling Burgers vectors by paths with glide and (sometimes partial) climb geometries. An example of pure climb paired $\tilde{5}$–$\tilde{7}$ disclination pairs is shown in Fig. 1*A*, where the vertices of the cut pattern are seen to lie on the dual lattice sites. In contrast, the vertices of the cut pattern for 2–4 pairs lie entirely on the honeycomb lattice and its basis; thus, in its folded configuration a 2–4 defect pair will appear as a pair of neighboring points on the honeycomb lattices with twofold and fourfold coordination (instead of the normal threefold). Another allowed kirigami motif is the sixon, a defect formed by completely removing one hexagon from the honeycomb lattice and reconnecting the cut edges of the remaining surface in one of several

Significance

How can flat surfaces be transformed into useful three-dimensional structures? Recent research on origami techniques has led to algorithmic solutions to the inverse design problem of prescribing a set of folds to form a desired target surface. The fold patterns generated are often very complex and so require a convoluted series of deformations from the flat to the folded state, making it difficult to implement these designs in self-assembling systems. We propose a design paradigm that employs lattice-based kirigami elements, combining the folding of origami with cutting and regluing techniques. We demonstrate that this leads to a pluripotent design in which a single kirigami pattern can be robustly manipulated into a variety of three-dimensional shapes.

Author contributions: D.M.S., Y.C., T.C., X.G., S.Y., and R.D.K. designed research; D.M.S., Y.C., T.C., X.G., E.J., and R.D.K. performed research; E.J. analyzed data; and D.M.S., Y.C., T.C., S.Y., and R.D.K. wrote the paper.

The authors declare no conflict of interest.

This article is a PNAS Direct Submission.

[1]D.M.S. and Y.C. contributed equally to this work.

[2]To whom correspondence should be addressed. Email: kamien@physics.upenn.edu.

This article contains supporting information online at www.pnas.org/lookup/suppl/doi:10.1073/pnas.1506048112/-/DCSupplemental.

PHYSICS

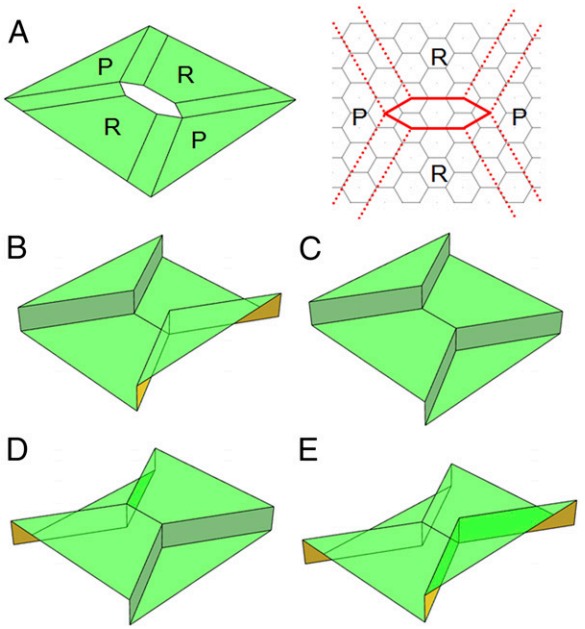

Fig. 1. Construction and configuration of the fundamental $\tilde{5}$–$\tilde{7}$ climb pair kirigami element. (*A*) The cut surface in its unfolded state with and without the underlying honeycomb lattice. Because they share an edge after assembly, regions marked "R" must be at the same height in the folded configuration. Regions marked "P" can either be at the same height or differ in height by two. (*B*–*E*) The four allowed folding configurations of the $\tilde{5}$–$\tilde{7}$ climb pair element.

degenerate ways. One configuration of the sixon identifies pairs of adjacent edges so that three triangular plateaus emanate from a central point; another configuration leads to matching 2–4 pairs in a pop-up/pop-down configuration (11).

In this paper we show that arrangements of these kirigami motifs enables a remarkably versatile ability to design patterns whose cut-and-folded state matches a desired target surface, allowing us to algorithmically solve the inverse design problem for a particular class of surfaces with a specified maximum gradient.

Importantly for their potential for self-assembly, the kirigami design paradigms we propose are both simple—to the extent of being easily designed by hand—and robust to the ordering and relative rates of edge folding. In what follows we will first describe a simple solution to the inverse design problem of creating a stepped surface with assigned heights at each point by arranging paired $\tilde{5}$–$\tilde{7}$ pairs along the lattice vectors of a larger superimposed honeycomb lattice. The excised patches define the location of the points of Gaussian curvature, and the designation of mountain and valley folds defines the height. We then present a second method using the same principle in a more refined manner to produce a reconfigurable surface. The stepped surfaces we create have many uses, among them being a similarity to water retention random surfaces in which the amount of water that collects in the basins of these landscapes is studied (15). Varying the parameters of the random landscape shows the link to percolation problems, and in this context our reconfigurable kirigami structures could be used to develop surfaces that can trigger the relevant percolation transition across the landscape in this and similar systems. More broadly, by invoking the degeneracy and flexibility of the sixon structure we can design a pluripotent lattice of sixons that can be folded into a dizzying array of target shapes by selectively assigning their mountain and valley folds.

Design Using $\tilde{5}$–$\tilde{7}$ Elements

Fig. 1 depicts a single $\tilde{5}$–$\tilde{7}$ climb pair element, where an extended hexagon is excised from the sheet, its edges are identified, and mountain and valley folds perpendicular to the short sides of the excised hexagon are applied. The two regions labeled "P" can independently pop up or pop down relative to their initial configuration, depending on the fold choices. In contrast, the regions labeled "R" share an edge in the folded configuration and therefore must be at the same height. Thus, an isolated $\tilde{5}$–$\tilde{7}$ climb pair element has four allowed configurations if we do not allow rotations in R^3.

A workable design paradigm requires combining many of these kirigami elements together, and in general one of the challenges of kirigami design is to understand the allowed relative configurations of kirigami elements. Important progress can be made by realizing that a collection of $\tilde{5}$–$\tilde{7}$ climb pair elements can be placed on the edges of a larger honeycomb superlattice, one

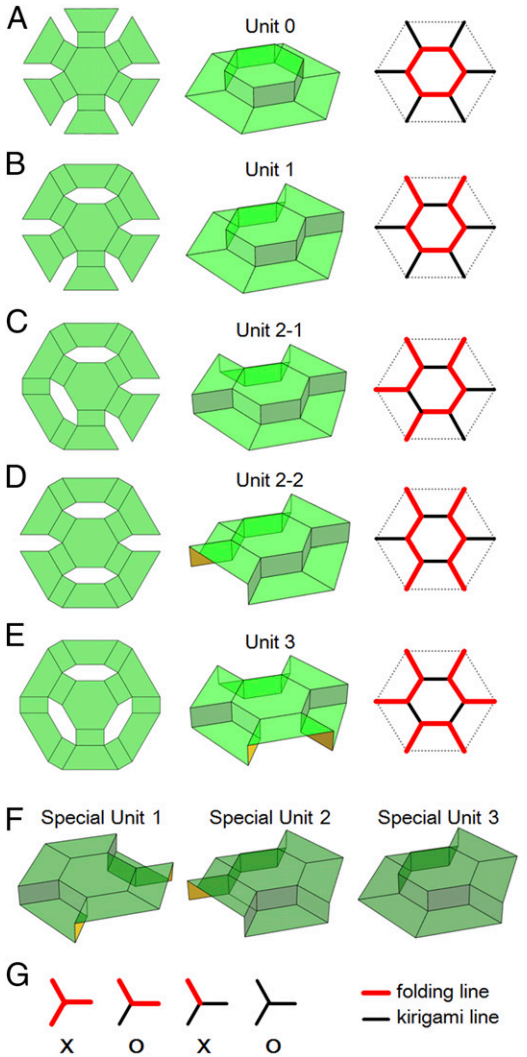

Fig. 2. (*A*–*E*) The basic building blocks of $\tilde{5}$–$\tilde{7}$ stepped surfaces. (*Left*) The unfolded configuration, where the excised hexagons sit on a larger-scale honeycomb lattice. (*Middle*) The folded configuration. (*Right*) A reduced representation suitable for easily designing target surfaces. (*F*) Folded configurations where the positive-climb paths of three dislocations converge. (*G*) Junction representation of the meeting of folding lines and cutting lines (i.e., places where excised regions had their edges identified) in the reduced representation. Only the junctions marked "O" represent allowed configurations.

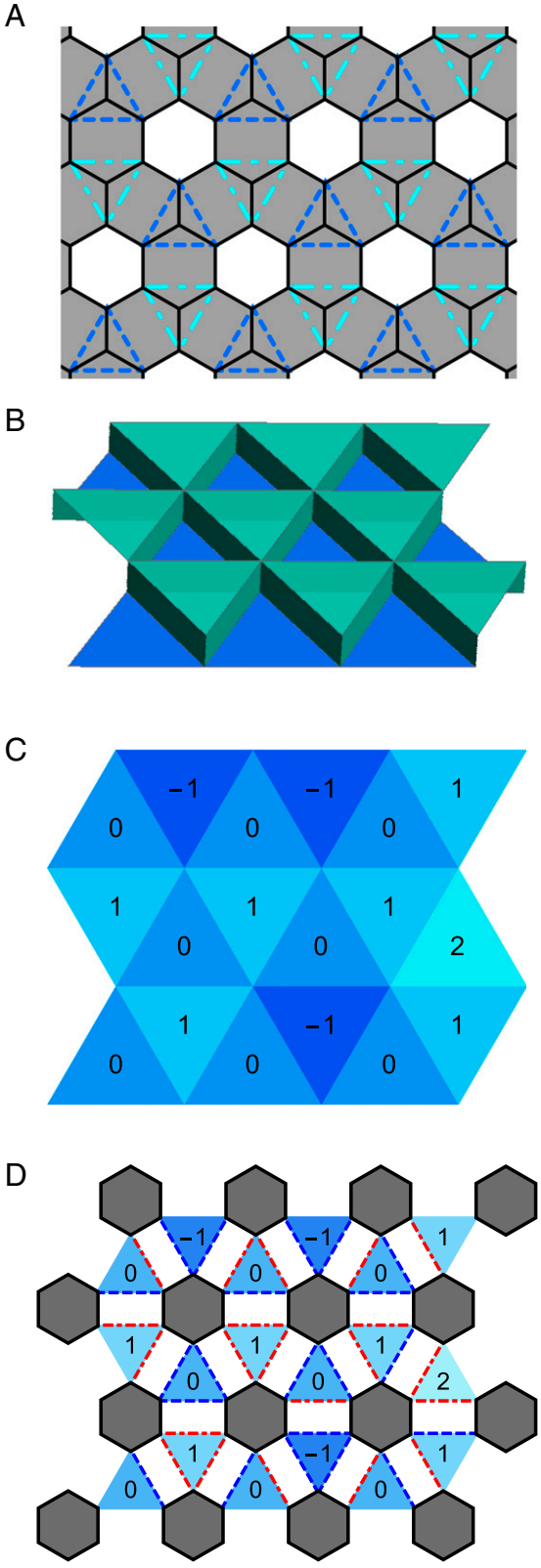

Fig. 3. (*A*) A triangular lattice of sixons together with lines for mountain (dot-dashed) and valley (dashed) folds to create the ground state configuration. (*B*) The ground state of the pattern in *A*, with sidewall heights reduced for visual clarity. (*C*) A reduced triangular representation for an arbitrary height configuration of the lattice, where the numbers inside each triangle correspond to the height of that triangular plateau. Each plateau height differs by one from any plateau with which it shares an edge. (*D*) The cut-and-fold pattern corresponding to the height map in *C*, where the gray hexagons are the excised regions.

whose edge lengths correspond to some multiple of the original lattice spacing. That is, arranging the $\tilde{5}$–$\tilde{7}$ cuts of the underlying lattice according to the superlattice positions guarantees that the kirigami elements are commensurate.

Fig. 2 *A*–*E*, *Left*, demonstrates the allowable ways (modulo rotations in R^3) of decorating a given hexagon in the bulk of the superlattice with $\tilde{5}$–$\tilde{7}$ elements (additional units are allowed at the boundaries of the sheet) while still maintaining the connectedness of the sheet. For instance, the structure labeled "Unit 0" is created with zero cuts and six folds around the central hexagon, which is accommodated by arranging six radial $\tilde{5}$–$\tilde{7}$ climb pair elements that each point at the corner of a hexagon on the superlattice. Fig. 2, *Middle*, shows the folded configuration of each of these basic building blocks. In our nomenclature, "Unit *n*" refers to a superlattice hexagon with *n* of its sides replaced with a $\tilde{5}$–$\tilde{7}$ climb pair element. The three structures in Fig. 2*F* labeled "special units" contain points at which three dislocations, whose Burgers vectors sum to zero, have positive-climb paths that converge together (as described in the Supplementary Material in ref. 11). In real materials these special units may be less stable than the other units, but their use substantially simplifies the design of target structures.

Fig. 2, *Right*, shows a simplified 2D representation of each structure given by color-coding the edges of the hexagonal superlattice as either folds or cuts (trivially done by comparing the relative elevation of the structure across a line). The allowable configurations can be determined by considering each vertex of the superlattice, as shown in Fig. 2*G*: to avoid tearing and other unwanted structural deformations of the sheet, each vertex must have either zero or two folding lines incident upon it.

With this junction rule in hand it is straightforward to reverse engineer a 2D map of the $\tilde{5}$–$\tilde{7}$ elements and fold lines needed to stepwise approximate a target surface. In *Supporting Information* we demonstrate this by designing a kirigami ziggurat, which we then realize in a simple experimental setting.

However, even aside from the restrictions imposed by the junction rules described above, these $\tilde{5}$–$\tilde{7}$ climb pair kirigami designs share one of the fundamental limitations of the origami patterns: for every desired target surface an entirely new pattern of cuts has to be programmed into the sheet, and only then can the folds be made. In many contexts we would prefer a pluripotent kirigami blueprint. Similar in spirit to the universal hinge pattern for making generic polycubes (16), we desire a single arrangement of kirigami elements that can accommodate many different target structures, all accessed by entirely local sequences of fold reassignments (i.e., changing a local set mountain folds to a valley folds and vice versa). In the next section we show that a triangular lattice of sixons can achieve precisely this goal.

Deploying Sixons for Surface Design

As before, to make use of the sixon structure we must understand the allowed arrangements of sixons with respect to each other. Fortunately, this is particularly straightforward: multiple sixons can be arranged in a triangular lattice. That is, the fold patterns required by the placement of multiple sixons can be made commensurate by choosing the excised hexagon centers to lie on a triangular lattice. The simplest implementation of this is shown in Fig. 3*A*. The folded state of this pattern, schematically shown in Fig. 3*B*, consists of triangular basins at height 0 separated by triangular plateaus at height 1 (in units of the sidewall heights). By thinking of this structure in a gravitational potential we consider the configuration in Fig. 3*B* to be the ground state of the triangular lattice of sixons because it minimizes the sum of the relative plateau heights.

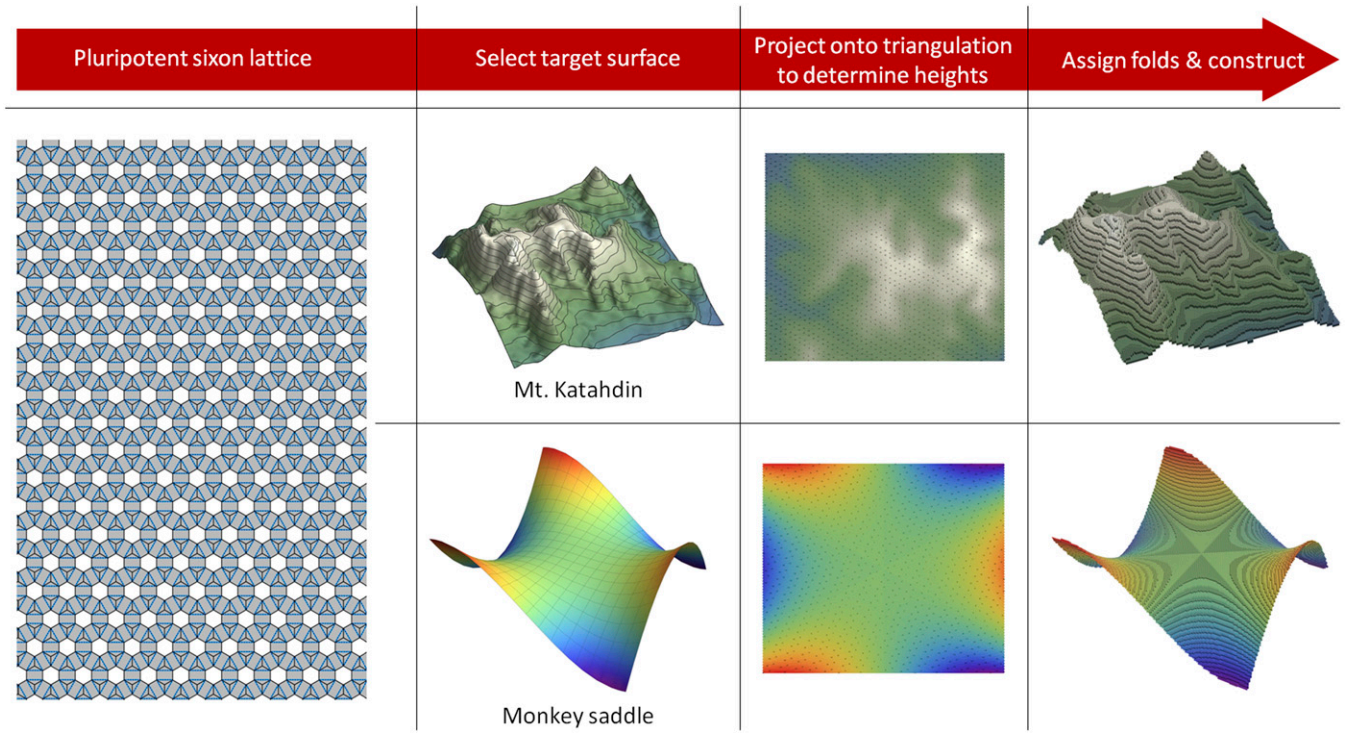

Fig. 4. Illustration of the pluripotent design capability of the sixon lattice. Starting from the base configuration of a 151 × 151 grid of triangular plateaus, a target surface is first selected [here a monkey saddle or Mt. Katahdin (18)]. The height of this target surface is projected onto the grid of triangular patches, and from this a local sequence of fold assignments is made to construct the final kirigami structure.

Local excitations of this configuration correspond to changing the plateau heights, for instance, by interchanging the nested valley and mountain folds around a height-zero triangular basin, creating a height-two triangular plateau surrounded by height-one plateaus. If the sheet can bend and stretch as in bistable origami (17), transforming from the ground state to these excited states only requires opening and then reclosing the three excised hexagons that bound the relevant triangular plateau. Otherwise, to avoid tearing or bending while moving from one target to another, it is necessary to return to the completely flat state. The requirements that folds be commensurate and the sheet not stretch impose the only restriction on allowed excitations: the height of any triangle in the folded configuration must differ by one from the height of any triangle with which it shares an edge. One such excited state is shown in Fig. 3*C*; as shown in Fig. 3*D*, given a reduced representation of the heights, it is trivial to assign the corresponding mountain and valley folds in the real sheet.

The restriction on the excited states is quite modest, making it easy to design a cut-and-fold pattern based on a triangular lattice of sixons that approximately matches a target surface with a stepped surface of triangular plateaus. In this formulation, achievable target surfaces are limited only to have a maximum gradient set by the ratio of plateau height to plateau width. If the gradient of the target surface obeys this bound, finding the kirigami solution to the inverse design problem is as straightforward as projecting the heights of a target surface down onto a triangular lattice and then rounding the height assignment of each triangle to the nearest even or odd integer so that triangles sharing an edge will have heights that differ by exactly one. Indeed, if there is a known maximum gradient among the target surfaces into which a sixon array will be (re)configured, the cut sizes determining the ratio of plateau height to width can be chosen to match this maximum gradient. From the triangular height map the pattern of mountain and valley folds immediately follows, as in Fig. 3*D*. We illustrate this simple design paradigm in Fig. 4, where the same triangular lattice of sixons can be used to approximate (to pick two arbitrary examples) both a monkey saddle and the topographic features at the northern terminus of the US Appalachian Trail (18).

Conclusion

We have demonstrated that adding kirigami cutting motifs to the folds of origami leads to a powerful framework in which target structures can be algorithmically designed via arrays of kirigami elements. Subject to a gradient constraint, using a superlattice simplifies the design for a static target surface, whereas triangular lattices of sixons form a versatile base pattern able to accommodate fold patterns for any stepped target structure. If the material allows for dynamic changing of fold type, then the sixon lattice can be reconfigured between arbitrary surface configurations. Current studies involve designing pluripotent kirigami templates that lift the gradient limitation as well as other geometric and topological limits. We note that our choice of triangular plateaus and sixons was a powerful but not entirely unique choice with which to engineer a pluripotent sheet of kirigami elements. We show in *Supporting Information* that using square plateaus leads to a similar (but more restrictive) design paradigm.

We note that our kirigami designs are superior to many origami designs for comparable results, especially in relation to self-assembly. For example, our experimental realization of a ziggurat-style pryamid (*Supporting Information*)—actuated by heat-shrink tape placed across the short axis of the excised hexagons—makes it clear that in our kirigami constructions the fold process is very robust. That is, in contrast with the origami methods discussed above, detailed control over the folds is not necessary to correctly form the target structure. Also, unlike some origami designs, this kirigami-based approach to approximating surfaces with sixons maintains a constant complexity of fold pattern per unit surface area. The underlying

structure is always a triangular lattice of sixons, and different surfaces differ in their folding template only by switching mountain and valley folds as needed.

Because the folds connecting sixons are coupled, a triangular lattice of sixons has more fold lines than degrees of freedom. This attribute could be exploited to create truly multipotent kirigami sheets by partitioning the folds into nonoverlapping sets and programming each of those sets to fold in response to different stimuli. We schematically illustrate such a duopotent sheet in *Supporting Information*, programming half of the fold lines to form a half-cylinder when activated, whereas the other half of the fold lines transform the sheet into a Mexican hat potential. This raises the exciting prospect that with dynamical control over the fold type, a single lattice of sixons could serve as the base for, e.g., microfluidic devices with dynamically changeable channels. Work on implementing such a dynamically reconfigurable kirigami surface is currently underway. We also anticipate that exploring the collective elasticity of these kirigami sheets will provide further insight into 2D mechanical metamaterials (19).

ACKNOWLEDGMENTS. Y.C. thanks Prof. D. J. Srolovitz for stimulating discussions and comments. The authors acknowledge support from National Science Foundation Emerging Frontiers in Research and Innovation - Origami Design for Integration of Self-assembling Systems for Engineering Innovation (NSF EFRI-ODISSEI) Grant EFRI 13-31583. D.M.S. was supported by the Advanced Materials Fellowship from the American Philosophical Society. This work was partially supported by a Simons Investigator Grant from the Simons Foundation (to R.D.K.).

1. Hamm CE, et al. (2003) Architecture and material properties of diatom shells provide effective mechanical protection. *Nature* 421(6925):841–843.
2. Klein Y, Efrati E, Sharon E (2007) Shaping of elastic sheets by prescription of non-Euclidean metrics. *Science* 315(5815):1116–1120.
3. Miura K (1980) Method of packaging and deployment of large membranes in space. *Proceedings of the 31st Congress of the International Astronautical Federation, IAF-80-A 31* (Am Inst Aeronaut Astronaut, New York), pp 1–10.
4. Mahadevan L, Rica S (2005) Self-organized origami. *Science* 307(5716):1740.
5. Borrelli V, Jabrane S, Lazarus F, Thibert B (2012) Flat tori in three-dimensional space and convex integration. *Proc Natl Acad Sci USA* 109(19):7218–7223.
6. Silverberg JL, et al. (2014) Applied origami. Using origami design principles to fold reprogrammable mechanical metamaterials. *Science* 345(6197):647–650.
7. Na J-H, et al. (2015) Programming reversibly self-folding origami with micropatterned photo-crosslinkable polymer trilayers. *Adv Mater* 27(1):79–85.
8. Lang RJ (1996) A computational algorithm for origami design. *Proceedings of the Twelfth Annual Symposium on Computational Geometry* (Assoc Comput Mach, New York), pp 98–105.
9. Tachi T (2009) 3D origami design based on tucking molecule. *Origami4* (CRC Press, Taylor & Francis Group, Boca Raton, FL), pp 259–272.
10. Tachi T (2010) Freeform variations of origami. *J Geom Graph* 14(2):203–215.
11. Castle T, et al. (2014) Making the cut: Lattice kirigami rules. *Phys Rev Lett* 113(24): 245502.
12. Sadoc J-F, Rivier N, Charvolin J (2012) Phyllotaxis: A non-conventional crystalline solution to packing efficiency in situations with radial symmetry. *Acta Crystallogr A* 68(4):470–483.
13. Charvolin J, Sadoc J-F (2011) A phyllotactic approach to the structure of collagen fibrils. *Biophys Rev Lett* 6(1):13–27.
14. Sadoc J-F, Charvolin J, Rivier N (2013) Phyllotaxis on surfaces of constant Gaussian curvature. *J Phys A Math Theor* 46(29):295202.
15. Knecht CL, Trump W, Ben-Avraham D, Ziff RM (2012) Retention capacity of random surfaces. *Phys Rev Lett* 108(4):045703.
16. Benbernou NM, Demaine ED, Demaine ML, Ovadya A (2011) Universal hinge patterns for folding orthogonal shapes. *Origami5* (CRC Press, Taylor & Francis Group, Boca Raton, FL), pp 405–419.
17. Silverberg JL, et al. (2015) Origami structures with a critical transition to bistability arising from hidden degrees of freedom. *Nat Mater* 14(4):389–393.
18. US Geological Survey (1999) Elevation data set n46w069sm (US Department of the Interior, Washington, DC).
19. Paulose J, Chen BG, Vitelli V (2015) Topological modes bound to dislocations in mechanical metamaterials. *Nat Phys* 11(2):153–156.